

# Modeling of the Slewing Control of a Flexible Structure

Ephraim Garcia\* and Daniel J. Inman†

State University of New York at Buffalo, Buffalo, New York 14260

This paper presents a formulation for the modeling of a single-link flexible beam that is undergoing slewing motion at an actively controlled pinned end, where the other end of the beam is free. This pinned end, or slewing axis, is of fixed orientation such that the beam rotates in the horizontal plane. A geared DC electric motor is connected to the beam at the slewing axis. A position and a velocity sensor are placed at this hinged location, and their proportional feedback provides a position control system about the slewing axis. The motor characteristics, gear ratio, and the position feedback constant determine an equivalent rotational spring constant, often called the servo stiffness. This paper generalizes the structure's boundary conditions at the slewing axis to include the effects of the servo system. It is shown that the clamped-free beam assumption for the dynamics of the structure is a valid assumption if the ratio of the servo stiffness to beam flexibility is high. However, for moderate or low values of this ratio, the clamped-free beam leads to erroneous system models so that it becomes necessary to consider the effects of the driving servo on the dynamics of the flexible beam.

## Nomenclature

$A_i$	= normalization constant of the $i$ th eigenfunction
$a_i L$	= $i$ th eigenvalue
$b_v$	= equivalent viscous damping
$c_v$	= viscous damping in the motor (bearing friction)
$D$	= damping matrix, closed-loop system
$E$	= elastic modulus
$EI$	= flexural rigidity
$e_a$	= voltage applied across the armature circuit
$I$	= cross-sectional moment of inertia
$I_b$	= rotatory inertia of the beam about the slewing axis
$I_m$	= motor inertia
$I_{n \times n}$	= $n \times n$ identity matrix
$i_a$	= current in the armature circuit
$J$	= equivalent rotatory inertia
$K$	= stiffness matrix, closed-loop system
$\bar{K}$	= stiffness matrix, open-loop system
$K_b$	= back electromotor force (emf) constant
$K_p$	= position feedback gain
$K_t$	= motor torque constant
$k$	= equivalent spring constant or servo stiffness
$L$	= beam length
$L_a$	= armature inductance
$M$	= inertia matrix, closed-loop system
$\bar{M}$	= inertia matrix, open-loop system
$N_g$	= gear ratio
$p(x, t)$	= beam loading
$q_i$	= $i$ th modal coordinate
$q$	= displacement vector
$R_a$	= armature resistance
$(\cdot)_x$	= differentiation with respect to $x$
$y(x, t)$	= deflection of the beam with respect to $x$
$\Gamma_i$	= modal participation factor of the $i$ th mode
$\delta'(x - x_0)$	= moment delta function acting at $x_0$
$\theta$	= angular position of the rigid body motion
$\theta'$	= total angular position of the beam
$\theta_m$	= angular position of the motor
$\rho$	= mass density per unit length

$\tau$	= torque applied to beam
$\tau_a$	= torque applied to gearbox
$\tau_e$	= restoring torque
$\phi_i(x)$	= $i$ th eigenfunction

## Introduction

THE current method of modeling the slewing control of flexible structures<sup>1,2</sup> is investigated. Slewing motion is the rotation of a structure about some point or axis. Some simple examples of slewing are a door that slews about its hinges and a solar panel pivoting about a point on a satellite. The slewing control of flexible structures has been studied by researchers in the area of large space structures.<sup>1,3-5</sup> Theoretically, the modeling of a slewing structure is similar to modeling a flexible single-link manipulator moving in the horizontal plane, which is also a current area of research in the robotics field.<sup>2,6-9</sup> A large number of problems can be classified as slewing problems, e.g., attitude maneuvers of rigid satellites. Much of the literature involving slewing of flexible structures has been on satellites with flexible appendages.<sup>3,5</sup> For the context of this paper, we will define slewing as a flexible structure torque driven about a pinned (or hinged) end.

In both robotics research and in the structural control communities, the simple one-link structure is usually modeled as a flexible beam fixed to a rotating axis. Modeling work performed by Hastings and Book<sup>2</sup> contains the open-loop transfer function of a single-link flexible manipulator arm carrying a tip load. This work uses an open-loop transfer function for verification of the natural frequencies of the beam predicted by Euler-Bernoulli beam theory for clamped-mass and pinned-mass boundary conditions. However, Hastings and Book<sup>2</sup> did not take into account the contribution of the driving motor's properties or the effects of the control on the boundary conditions for the beam's eigenanalysis. That is to say, geometric rather than natural boundary conditions were used for the eigenanalysis of the structure.

Typically a position, or servo, control system is used at the slewing axis for precise maneuvering or pointing control. Although this collocated sensor and actuator is arguably the simplest position control system, it requires that we reconsider the effects of the control on the dynamics of slewing flexible structures. Book and Majette<sup>6</sup> considered the effects of a compliant servo system, where the structural vibrations cause a rotation about the point of rotation, i.e., the beam was not assumed to be clamped at the slewing axis. The effects of the servo were considered to be that of a spring and a rotational damper at the point of rotation. The main difference between

Received June 5, 1989; revision received April 30, 1990; accepted for publication May 7, 1990. Copyright © 1990 by the American Institute of Aeronautics and Astronautics, Inc. All rights reserved.

\*Research Assistant Professor, Department of Mechanical and Aerospace Engineering. Member AIAA.

†Professor and Chair, Department of Mechanical and Aerospace Engineering. Member AIAA.

this work and Ref. 6 is that this work is formulated using the Ritz method, or modal summation procedure for the dynamics of the structure as opposed to the frequency domain approach of Ref. 6.

The premise of this paper is that the positioning control system used for the maneuvering of the flexible structure determines the boundary conditions for the vibratory motion of the structure. Although obvious, this statement alters the usual effect of feedback on the system dynamics. In control theory, the plant is often considered to be the open-loop model to which some feedback and control inputs are added, thus changing the overall response of the system. The plant in this case is a flexible structure that is slewed about an axis. If we accept the fact that the feedback parameters determine the boundary conditions (hence, the dynamics of the structure), then not only does the response of the overall system vary with feedback, but the plant dynamics depend on the control law.

The effects of the servo controller on the beam, as felt by the beam, can be modeled as a spring, where the actuator parameters and position feedback gain determine the spring rate constant. This equivalent rotational spring is normally referred to as the servo stiffness. These gains are large for some applications of control of flexible structures. This provides a fast response servo-positioning system that is usually required for robotic applications in manufacturing or a fast response for the flexible appendages of strategic satellites. It will be shown that in these high gain applications where the ratio of servo stiffness  $k$  to beam flexibility  $EI/L$  is large, the clamped-free assumption is valid. However, when  $kL/EI$  is moderate or small, it will be shown that the beam does not behave in a clamped-free fashion.

Consider the effects of a motor-actuated servo system acting at the slewing axis on the vibratory motion of the flexible structure. The torque generated by the vibrating structure is opposed by rotational stiffness of the servo system. In addition to the effects, the properties of the motor, i.e., the inertia, back electromotor force (EMF) and viscous damping are also considered in the boundary conditions. Assuming that the servo stiffness is the dominant of the three torques, this paper considers the effects of the servo stiffness in the eigenanalysis of the structure rather than assuming that the beam is clamped. The effects of the spring at the boundary yields a more precise dynamic model of the slewing control of a flexible structure.

### Model Development

The following is a formulation of the dynamics of a controlled single-link flexible structure that is mounted on a rotating axis. The beam in Fig. 1 is pinned at point A, the slewing axis, where a torque  $\tau$  is applied. The assumptions made in developing the equations of motion for the system are those of small vibration theory. The rotatory inertia of the beam is assumed to be small, and the shear deformation is ignored. Additionally, the inertia and radius of the hub are small, hence, the effects of the hub are not included in the dynamics. In general, the hub effects can be included in our model by adding an equivalent inertia to our motor. The beam is moving in the horizontal plane so that gravity effects are not included. The properties  $EI$  and  $\rho$  are constant over the beam's length,  $L$ .

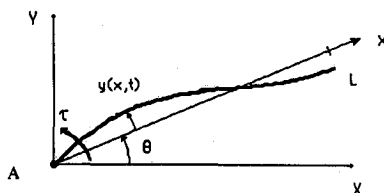


Fig. 1 Slewing flexible beam—top view.

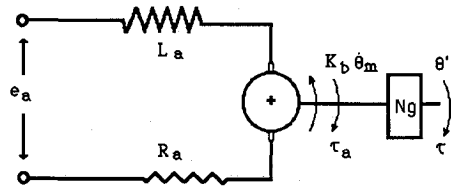


Fig. 2 Motor armature circuit and gearbox schematic.

The effects of centripetal stiffening have been included previously in modeling flexible structures<sup>4,10,11</sup>; centripetal stiffening leads to a nonlinear model. While those effects may be significant for high slewing rates, the goal of this analysis is to consider the effects of the control on the eigenanalysis of the structure and, from this, generate a linear model for the system. Those centripetal effects limit the use of this analysis to fast slewing maneuvers.

### Open-Loop Dynamics

The equations of motion for the flexible beam about a rotating axis are derived using Hamilton's principle. At this point we do not consider the effects of the motor and servo control. The Lagrangian of this system is

$$L_g = \frac{1}{2} \int_0^L \rho (\dot{x} \dot{\theta} + \dot{y})^2 dx - \frac{1}{2} \int_0^L EI \left( \frac{\partial^2 y}{\partial x^2} \right)^2 dx \quad (1)$$

and consists of the total kinetic energy of the beam minus the total potential or strain energy of the structure. The expression for the total kinetic energy in Eq. (1) is actually an approximation that is valid in the realm of small vibration theory. The nonconservative work performed on this system by the applied torque is

$$W_{nc} = \tau \theta + \tau \frac{\partial y(0,t)}{\partial x} \quad (2)$$

where  $\theta$  is the displacement of the system in its rigid body mode, and  $\partial y(0,t)/\partial x$  that is the angular displacement of the beam with respect to the axis defining rigid body displacement. Applying Hamilton's principle,

$$\delta \int_{t_1}^{t_2} (L_g + W_{nc}) dt = 0 \quad (3)$$

we obtain the following integral expressions,

$$\int_0^L \left( EI \frac{\partial^4 y}{\partial x^4} + \rho \ddot{y} + \rho x \ddot{\theta} \right) dx = 0 \quad (4)$$

$$\int_0^L [\rho x (\ddot{x} \dot{\theta} + \dot{y})] dx = \tau \quad (5)$$

and the following boundary conditions:

At  $x = L$

$$EI \frac{\partial^2 y}{\partial x^2} = 0, \quad \frac{\partial}{\partial x} EI \frac{\partial^2 y}{\partial x^2} = 0 \quad (6a)$$

At  $x = 0$

$$EI \frac{\partial^2 y}{\partial x^2} - \tau = 0, \quad y = 0 \quad (6b)$$

A separation of variables solution for the motion of the beam is assumed, i.e.,

$$y(x,t) = \sum_{i=1}^n q_i(t) \phi_i(x) \quad (7)$$

where  $n$  is a finite number equal to the number of structural modes of vibration included in our model, and the terms  $q_i$  are the modal coordinates of the structure. Substituting Eq. (7)

into Eq. (5), we obtain the equation of motion for the rigid body mode of the system:

$$I_b \ddot{\theta} + \sum_{i=1}^n I_i \ddot{q}_i = \tau \quad (8)$$

where

$$I_b = \int_0^L \rho x^2 dx \quad I_i = \int_0^L \rho x \phi_i(x) dx$$

and where  $I_b$  is the inertia of the rigid beam about the slewing axis, and  $I_i$  is the modal inertia due to the flexibility of the beam. Substituting Eq. (7) into Eq. (4),  $n$  more equations are obtained for the structural modes of the beam:

$$\int_0^L \rho \phi_i(x) \phi_j(x) dx \ddot{q}_i + \int_0^L EI \phi_{i,xxxx}(x) \phi_j(x) dx q_i = -I_i \ddot{\theta} \quad (9)$$

It is assumed that the eigenfunctions are orthogonal and adhere to the following orthogonality relationships<sup>10</sup>:

$$\int_L \rho \phi_i \phi_j dx = \delta_{ij} \quad (10a)$$

$$\int_L EI \frac{\partial^4 \phi_i}{\partial x^4} \phi_j dx = \omega_i^2 \int_L \rho \phi_i \phi_j dx \quad (10b)$$

Applying Eqs. (10a) and (10b), the following matrix equation is obtained for the  $n + 1$  open-loop equations of motion:

$$\tilde{M} \ddot{q} + \tilde{K} q = B \tau \quad (11)$$

where

$$\tilde{M} = \begin{bmatrix} I_b & I_1 & \cdots & I_n \\ I_1 & & & \\ \vdots & & I_{n \times n} & \\ I_n & & & \end{bmatrix}$$

$$\tilde{K} = \begin{bmatrix} 0 & \mathbf{0}_{1 \times n} \\ \mathbf{0}_{n \times 1} & \text{DIAG} \{ \omega_1^2, \dots, \omega_n^2 \} \end{bmatrix}$$

$$q^T = [\theta, q_1, \dots, q_n], \quad B^T = [1, 0, \dots, 0]$$

Most often in the literature<sup>1,2</sup> the eigenfunctions  $\phi_i(x)$  are chosen as those that satisfy the Euler-Bernoulli equation with the clamped-free conditions, i.e., at the fixed end the displacement and slope vanish, and at the free end the moment and shear vanish. The use of the clamped-free eigensolution usually stems from the argument that the beam is clamped to the axis, and indeed it is; however, the axis is free to rotate. Thus, we observe that the open-loop behavior of the structure would appear to be that of a pinned-free beam rather than that of a clamped-free beam (neglecting the inertia of the axis). If we substitute the eigenfunctions for a pinned-free beam (see Table 1) into the inertia matrix  $\tilde{M}$  of Eq. (11), the off-diagonal terms become,

$$I_i = \int_0^L \rho x \phi_i(x) dx = C_i [\tan(a_i L) - \tanh(a_i L)] = 0 \quad (12)$$

where  $C_i$  depends on the value of the eigenvalues. The right-hand side of Eq. (12) is the eigenvalue equation for a pinned-free beam (see Table 1). This results in zero inertia terms due

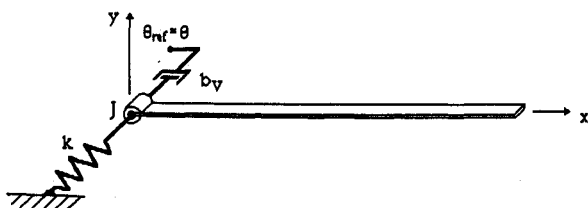


Fig. 3 Flexible beam with boundary conditions.

Table 1 Eigenfunctions for various boundary conditions

Boundary conditions	Eigenfunctions and corresponding eigenvalue equations
Pinned-free	$\phi_i(x) = A_i \begin{bmatrix} \cosh(a_i L) & \sin(a_i x) + \sinh(a_i x) \\ \cos(a_i L) & \end{bmatrix}$ $\tan(a_i L) = \tanh(a_i L)$
Clamped-free	$\phi_i(x) = A_i \{ [\sin(a_i L) - \sinh(a_i L)][\sin(a_i x) - \sinh(a_i x)] + [\cos(a_i L) + \cosh(a_i L)][\cos(a_i x) - \cosh(a_i x)] \}$ $\cos(a_i L) \cosh(a_i L) + 1 = 0$
Pinned/spring-free	$\phi_i(x) = A_i \left\{ -\frac{C_{1i}}{C_{2i}} \sin(a_i x) + \sinh(a_i x) + \frac{k'}{a_i L} \left( 1 - \frac{C_{1i}}{C_{2i}} \right) [\cosh(a_i x) - \cos(a_i x)] \right\}$ <p>where</p> $k' = \frac{1}{2} \frac{kL}{EI}$ $C_{1i} = \frac{k'}{a_i L} [\sinh(a_i L) - \sin(a_i L)] + \cosh(a_i L)$ $C_{2i} = \frac{k'}{a_i L} [\sinh(a_i L) - \sin(a_i L)] - \cos(a_i L)$ $\frac{EI}{kL} a_i L [\sinh(a_i L) \cosh(a_i L) - \cos(a_i L) \sinh(a_i L)] = \cos(a_i L) \cosh(a_i L) + 1$

to the flexible modes, i.e.,  $I_i = 0$  for all  $i = 1, \dots, \infty$ , and an uncoupled system whose rigid body motion has no coupling to the flexible motion of the structure. This uncoupled system is not meaningful from our observations and intuition. Intuitively, we know that as torque is applied at the slewing axis, the bending of the flexible modes occurs due to the angular acceleration of the rigid body motion. This phenomena is represented by the off-diagonal terms of the mass matrix. Equation (12) shows that this inertia coupling disappears when a pinned-free beam eigensolution is used for the dynamics of the beam. The use of eigenfunctions with the pinned boundary conditions at the slewing axis of the structure leads to erroneous system models as pointed out by Hastings and Book.<sup>2</sup>

The eigensolution of the beam is, of course, determined by the boundary conditions. However, the boundary conditions at the root of the beam are not determined by the open-loop system. The boundary conditions at the slewing axis are affected by the position control system itself. The rotation that occurs at the axis due to the beam vibrations is dependent largely on the stiffness of the servo system. The servo stiffness is assumed to behave as a rotational spring at the boundary of the beam. For instance, if no position feedback was applied, the system in Fig. 1 would behave as a pinned-free beam; i.e., the structure at the axis would be unconstrained by the control. Therefore, to determine the correct eigenfunctions, we must understand the relationship between the motion of the beam and the governing control law.

#### Actuator Dynamics

The torque applied to the beam is considered here to be generated by an armature-controlled DC electric motor, whose behavior is represented by the schematic in Fig. 2. Applying Kirchhoff's voltage law to the circuit, we obtain

$$e_a = i_a R_a + L_a \frac{di_a}{dt} + K_b \dot{\theta}_m \quad (13)$$

Table 2 Eigenvalues of a pinned/spring-free beam

$kL/EI$	$a_1L$	$a_2L$	$a_3L$	$a_4L$
Pinned-free				
$kL/EI \rightarrow 0$	0.0	3.9266	7.0686	10.2101
0.001	0.2340	3.9267	7.0691	10.2103
0.01	0.4159	3.9278	7.0693	10.2107
0.1	0.7358	3.9385	7.0756	10.2150
1.0	1.2479	4.0311	7.1341	10.2566
10	1.7227	4.3995	7.4510	10.5218
100	1.8568	4.6497	7.7827	10.8976
1000	1.8732	4.6894	7.8470	10.9847
Clamped-free				
$kL/EI \rightarrow \infty$	1.8751	4.6941	7.8548	10.9955

The sum of the torques about the motor armature yields

$$I_m \ddot{\theta}_m + c_v \dot{\theta}_m + \tau_a = K_t i_a \quad (14)$$

where  $\tau_a$  is the torque applied to the gearbox, and  $\theta_m$  is the angular position of the motor. The motion of the motor and the torque applied to the gearbox are related to the beam motion and the torque applied to the beam by

$$\tau = N_g \tau_a \quad (15a)$$

$$\theta_m = N_g \theta' \quad (15b)$$

where the total angular displacement is  $\theta'$ . Equations (13) and (14) are now combined by substituting with the relationships in Eqs. (15a) and (15b). The following expression for the torque applied to the beam in terms of the voltage applied to the armature circuit is

$$\tau = \frac{N_g K_t}{R_a} e_a - I_m N_g^2 \ddot{\theta}' - \left( c_v + \frac{K_b K_t}{R_a} \right) N_g^2 \dot{\theta}' \quad (16)$$

where we have assumed that the motor inductance is small.

#### Closed-Loop Response

For the closed-loop response, we set the armature voltage proportional to the error signal generated by the difference between a reference signal  $\theta_{ref}$  and the measured beam position; i.e.,

$$e_a = K_p \left\{ \theta_{ref} - \left[ \theta + \frac{\partial y(0,t)}{\partial x} \right] \right\} \quad (17)$$

Torque shaping,<sup>1</sup> which is the passing of the position error signal through a low-pass filter, is used to reduce the amount of vibratory motion imparted to the structure by the motor. With torque shaping, Eq. (17) would reduce to  $e_a = (\theta_{ref} - \theta)$ , but the effects of the beam's vibrations on the error signal are retained here for completeness. Combining Eq. (16) with Eq. (17), we obtain

$$\tau = k \theta_{ref} - k \left[ \theta + \sum_{i=1}^n \frac{\partial \phi_i(0)}{\partial x} q_i \right] - I_m N_g^2 \ddot{\theta} - \left( c_v + \frac{K_b K_t}{R_a} \right) N_g^2 \dot{\theta} \quad (18)$$

The term  $k = N_g K_p K_t / R_a$  is defined as the servo stiffness for the system. It has been assumed in Eq. (18) that the contribution of the actuator dynamics, the motor inertia, and servo damping due to the local rotational displacement  $\partial y(0,t)/\partial x$  is small. Equation (18) is now combined with the open-loop dynamics of Eq. (11) to obtain the equations of motion for the closed-loop response; namely,

$$M \ddot{q} + D \dot{q} + K q = B \theta_{ref} \quad (19)$$

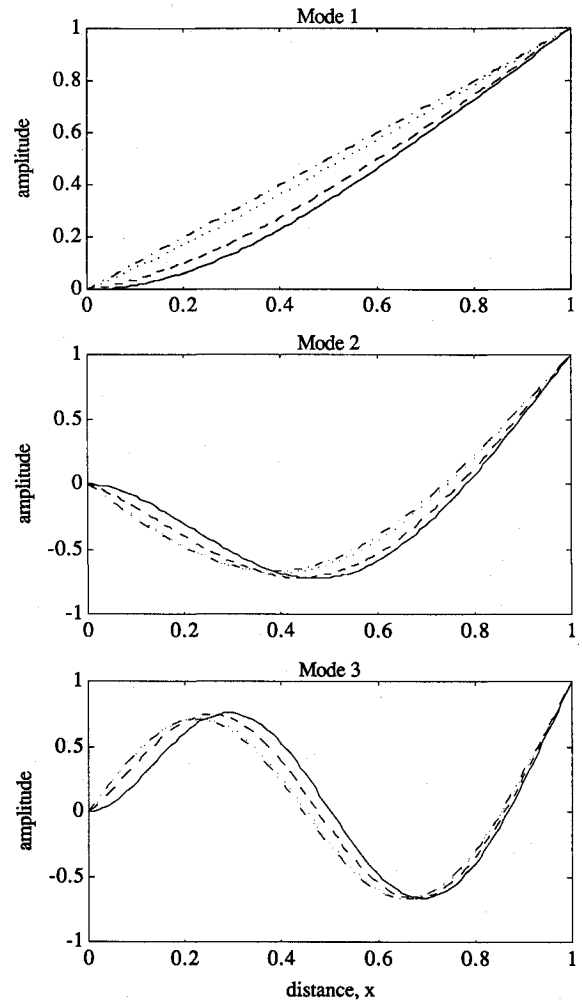


Fig. 4 Modes of vibrations for varying compliance ratios where  $kL/EI = 10^3$  (—), 10 (---), 1 (....), and  $10^{-2}$  (-.-.-).

where

$$M = \tilde{M} + \begin{bmatrix} I_m N_g^2 & \mathbf{0}_{1 \times n} \\ \mathbf{0}_{n \times 1} & \mathbf{0}_{n \times n} \end{bmatrix}$$

$$D = \begin{bmatrix} (c_v + K_b K_t / R_a) N_g^2 & \mathbf{0}_{1 \times n} \\ \mathbf{0}_{n \times 1} & \mathbf{0}_{n \times n} \end{bmatrix}$$

$$K = \tilde{K} + \begin{bmatrix} k & k \begin{bmatrix} \frac{\partial \phi_1}{\partial x} & \dots & \frac{\partial \phi_n}{\partial x} \end{bmatrix} \\ \mathbf{0}_{n \times 1} & \mathbf{0}_{n \times n} \end{bmatrix}$$

and

$$B^T = [k, \mathbf{0}_{1 \times n}]$$

Up to this point, the eigensolution of the structure has not been computed, but rather eigenfunctions are assumed to exist that satisfy the orthogonality conditions and converge to the solution. The eigensolution of the beam with control dependent boundary conditions is determined in the following section.

#### Eigenanalysis

Consider the vibratory motion of the controlled beam about some equilibrium so that  $\theta_{ref} = \theta$ . Imposing the boundary conditions of Eq. (6b) and the actuator dynamics of Eq. (18), it is proposed that the effects of the motor and servo control system on the beam are equivalent to the following parameter

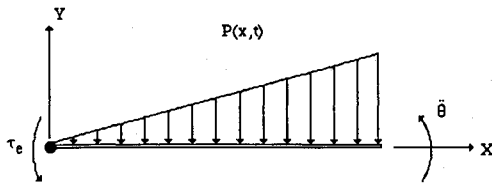
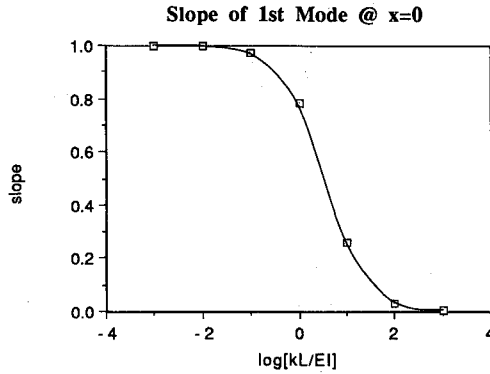


Fig. 5 Flexible beam with inertial load.

Fig. 6  $[\partial\phi(0)/\partial x]$  as normalized in Fig. 4.

model acting through the slewing axis of the beam depicted in Fig. 3, where  $b_v = (c_v + K_b K_i / R_a) N_g^2$  is a rotational viscous damper due to the viscous damping (the bearing friction)  $c_v$ , the back EMF of the motor  $K_b$ ,  $J = I_m N_g^2$  is a rotational inertia due to the motor acting through the gear ratio at the slewing axis, and  $k = N_g K_p K_i / R_a$  is the rotational spring constant due to the servo stiffness. Thus, by taking the sum of the moments at  $x = 0$ , the boundary conditions of the vibrating beam at the slewing axis become

At  $x = 0$ :

$$y(0, t) = 0 \quad (20a)$$

$$EI \frac{\partial^2 y(0, t)}{\partial x^2} = k \frac{\partial y(0, t)}{\partial x} + b_v \frac{\partial^2 y(0, t)}{\partial x \partial t} + J \frac{\partial^3 y(0, t)}{\partial x \partial t^2} \quad (20b)$$

Equations (20a) and (20b) are the generalized boundary conditions for the vibratory motion of a servo-controlled flexible beam with collocated position sensor and actuator acting at the slewing axis.

By assuming that the dissipative torque is small compared to the restoring torque of the servo stiffness, the viscous damping term  $b_v$  may be neglected in our boundary conditions. Additionally, for this eigenanalysis it is assumed that the motor inertia term is small. Neglecting the effects of the actuator must be done with the precaution that the neglected terms affect the boundary conditions with the square of the gear ratio.

Using the boundary conditions of Eq. (20) for the controlled end and free boundary conditions at the other end,<sup>12</sup> the eigenvalues of this spring-free beam are obtained (Table 1). Table 2 contains the eigenvalues of a spring-free beam for the range of values  $0.001 < kL/EI < 1000.0$ , and the corresponding eigenfunctions for the first three modes are plotted in Fig. 4. The problem of a beam with one end constrained by a pinned-spring condition and the other end free was first reported by Chun<sup>13</sup> and can also be found in Ref. 14.

It can be shown that, in the limit, as  $kL/EI \rightarrow \infty$ , the eigen-solution of the spring-free beam approaches that of a cantilevered beam, and as  $kL/EI \rightarrow 0$ , the eigenvalues and eigenfunctions of the spring-free approach those of a pinned-free beam. The final observation we make is that for a constant value of  $kL/EI$ , as the eigenvalues  $a_i L$  become large, the eigensolution of a pinned/spring-free system approaches that of a pinned-free beam. This last observation indicates that the

mode shapes and natural frequencies of the lowest few modes are the ones most affected by the spring-free boundary conditions, as expected. These are the modes that interact most strongly with the rigid body motion of the slewing maneuver and therefore are of particular importance. The term  $kL/EI$  is defined as the "compliance ratio," that is, the ratio between the servo stiffness  $k$  and the beam's normalized flexural rigidity  $EI/L$ .

### Implications of the Pinned Spring-Free Eigensolution

Intuitively, the idea of the servo stiffness determining the boundary conditions of the beam seems reasonable. But what are the implications of this eigenanalysis in terms of dynamic modeling? It can be expected that for the same number of mode shapes, this eigenanalysis would lead to a more accurate prediction of the beam's modal parameters (the natural frequencies and mode shapes), since we have applied the natural boundary conditions instead of the simpler geometric ones. More importantly, this analysis models the interaction between the actuator and the structure, i.e., the modal participation factors  $\Gamma_i(0)$ . The mode shapes associated with the natural boundary conditions account for the rotation at the slewing axis due to the beam flexure. This effect has been included in the closed-loop model of Eq. (19) through the off-diagonal terms of the stiffness matrix. This is in contrast to the clamped-free modal assumption whose modal participation factors are zero, thus yielding no off-diagonal terms. We must now reconsider the results of Hamilton's principle used to derive the open-loop equations of motion, Eq. (11).

The structure's motion with respect to the rotating  $x$  axis can be described by the following Euler-Bernoulli partial differential equation:

$$EI \frac{\partial^4 y(x, t)}{\partial x^4} = -\rho \frac{\partial^2 y(x, t)}{\partial t^2} + p(x, t) \quad (21)$$

and the appropriate boundary conditions.

The open-loop equations of motion for the flexible motion of the structure [Eq. (11), for  $q_1 - q_n$ ] are the same as those derived as if the load acting on the beam in Eq. (21) were an inertial load due to the angular acceleration of the rigid body motion, as indicated in Fig. 5. This inertial load can be stated as

$$p(x, t) = -\rho x \ddot{\theta}(t) \quad (22)$$

We now apply the modal transformation to Eq. (21); that is, we substitute Eq. (7) into Eq. (21) and use the loading defined in Eq. (22); then we multiply by the eigenfunction and integrate over the domain to arrive at

$$\ddot{q}_i + \omega_i^2 q_i = - \int_0^L \rho x \phi_i(x) dx \ddot{\theta}(t) = -I_i \ddot{\theta}(t) \quad (23)$$

The expression on the right-hand side corresponds to the coupling terms of the inertia matrix for the equations of motion, Eq. (11). Equation (23) represents the same equations of motion for the flexible motion of the structure as those derived in Eq. (11) using variational principles. Clearly, from Fig. 5 we can say that, in addition to the inertial load, there is an additional load due to the control's restoring torque  $\tau_e$  applied to the beam at the axis of rotation. We call this loading,

$$p(x, t) = \tau_e \delta'(x - x_0) - \rho x \ddot{\theta}(t) \quad x_0 = 0 \quad (24)$$

Then transforming to modal coordinates, we get

$$\ddot{q}_i + \omega_i^2 q_i = \Gamma_i(0) \tau_e - I_i \ddot{\theta}(t) \quad (25)$$

where

$$\Gamma_i(0) = \frac{\partial \phi_i(0)}{\partial x}$$

The new term in the equations of motion for the flexible structure Eq. (25) is  $\Gamma_i(0)$  and is known as the modal participation factor for the  $i$ th mode.<sup>12,15</sup> For the clamped-free eigenfunctions,  $\Gamma_i(0) = 0$ , by the definition of the clamped boundary condition. However, for the spring-free eigenfunctions, the modal participation factors of the restoring torque are not equal to zero, and this direct transmission of the restoring torque to the modal deflections must be included in our model. The restoring torque  $\tau_e$  is the torque due to the error signal multiplied by the feedback gain, i.e.,

$$\tau_e = k\theta_{\text{ref}} - k \left[ \theta + \sum_{i=1}^n \frac{\partial \phi_i(0)}{\partial x} q_i \right] \quad (26)$$

Specifically, this affects the control matrix  $B$  and the stiffness matrix  $K$  from Eq. (19); i.e., the control matrix is

$$B^T = \frac{N_g K_t K_p}{R_a} [1.0, \Gamma_1(0), \dots, \Gamma_n(0)] \quad (27)$$

where the modal participation factors have been included. Similarly, the stiffness matrix becomes

$$K = \begin{bmatrix} k & k[\Gamma_1(0) \cdots \Gamma_n(0)] \\ k\Gamma_1(0) & \\ \vdots & \text{DIAG}\{\omega_1^2 \cdots \omega_n^2\} \\ k\Gamma_n(0) & \end{bmatrix} \quad (28)$$

where the terms  $[\partial \phi_i(0)/\partial x]^2$  are considered to be of second order. This shows that when the compliance ratio is not large, the slope of the modes at the slewing axis are nonzero and generate nonzero values for the modal participation factors of the beam. Thus, Eqs. (26) and (27) contribute new terms to the control matrix  $B$  and the closed-loop stiffness matrix  $K$ .

The inclusion of modal participation factors is a generalization of the model derived in Ref. 1. If the compliance ratio is large, the eigensolution of the structure approaches that of clamped-free beam; hence the modal participation factors go to zero, and the model of Eq. (19) with the coefficient matrices of Eqs. (26) and (27) have the same form as the matrices of the model in Ref. 1.

### Systems with Small Compliance Ratios

The model derived in Eq. (19) with the additional terms from Eqs. (26) and (27) constitute a generalized model for the system in Fig. 1, where the effects of the control on the dynamics of the beam are included. However, a problem arises for this model for low values of the compliance ratio  $kL/EI$ . A low value of compliance ratio is defined when the first mode of the pinned/spring-free beam approaches the rigid body motion of the flexible structure, i.e., the first mode shape becomes a straight line (see Fig. 4). This leads to a mass matrix that is no longer positive definite, but as  $kL/EI$  becomes small, the mass matrix becomes positive semidefinite<sup>12</sup> and singular.

To show this, it is assumed that as  $kL/EI$  becomes small but is still nonzero and that the first eigenfunction of the pinned/spring-free beam approaches that of a straight line, i.e.,

$$\phi_1(x) \cong \sqrt{\frac{3}{\rho L^3}} x \quad (29)$$

where we have applied the orthogonality condition of Eq. (10a). The mode shape of Eq. (29) represents the rigid body motion. This rigid body motion differs from the rigid body mode in that the eigenvalue is nonzero. Noting that  $I_b = (\rho L^3/3)$ , the first principle minor of the mass matrix goes to zero as  $kL/EI$  becomes small, i.e.,

$$I_b - I_1^2 \rightarrow 0 \quad (30)$$

For a one-mode expansion, the first principle minor is also the value of the matrix determinant, so as  $kL/EI$  becomes small, the mass matrix becomes positive semidefinite and singular. This can be explained simply by the fact that as the first mode of the spring-free beam approaches the rigid body motion of the structure,  $q_1$  and  $\theta$  represent the same motion of the structure. Since these two variables are no longer independent, we need to collapse the model by one degree of freedom. For the case of small compliance ratio, the motion of the structure can be described by the flexible modes of a spring-free beam,  $\phi_2(x)$  to  $\phi_n(x)$ , and the rigid body motion whose position is represented by the angle  $\theta$ .

However, there is another consequence of the first mode of the spring-free beam approaching the rigid body motion of the beam. Since the eigenfunctions of the pinned/spring-free beam are orthogonal to each other, the coupling in the inertia matrix of Eq. (19) vanishes, as shown in Eq. (12). To clarify this, consider the following: as  $kL/EI$  becomes small (but nonzero), then  $\phi_1$  is proportional to the function  $x$ , Eq. (29). The modes  $(\phi_2, \dots, \phi_n)$  are the flexible modes of the weak spring-free beam and are approaching the flexible modes of the pinned-free beam. Since the modes  $(\phi_2, \dots, \phi_n)$  are orthogonal to the rigid body mode (a straight line), then they must also be orthogonal to the inertial loading term of Eq. (23). This inertial loading of the flexible modes generates the coupling terms of the inertia matrix. Hence, the terms  $I_2$  to  $I_n$  go to zero as  $kL/EI$  becomes small. It follows that the correct model for a small compliance ratio is that of Eq. (19) with the following coefficient matrices:

$$M = \begin{bmatrix} I_b & \mathbf{0}_{1 \times n-1} \\ \mathbf{0}_{n-1 \times 1} & I_{n-1 \times n-1} \end{bmatrix} \quad (31a)$$

$$D = \begin{bmatrix} (c_v + K_b K_t / R_a) N_g^2 & \mathbf{0}_{1 \times n-1} \\ \mathbf{0}_{n-1 \times 1} & \mathbf{0}_{n-1 \times n-1} \end{bmatrix} \quad (31b)$$

$$K = \begin{bmatrix} k & k[\Gamma_2 \cdots \Gamma_n] \\ k \begin{Bmatrix} \Gamma_2 \\ \vdots \\ \Gamma_n \end{Bmatrix} & \text{DIAG}(\omega_2^2, \dots, \omega_n^2) \end{bmatrix} \quad (31c)$$

$$B^T = \frac{N_g K_t K_p}{R_a} [1.0, \Gamma_2, \dots, \Gamma_n] \quad (31d)$$

where the modal coordinate  $q_1$  has been dropped. This model, Eq. (19), with the coefficients of Eqs. (31a-31d), is a very different model than if we had used a clamped-free assumption for the boundary conditions. Here the eigenfunctions and natural frequencies are those of the flexible modes of a nearly pinned-free beam. This results in stiffness coupling through the modal participation factor and the position feedback rather than in the mass matrix.

### Summary

We have shown that for a range of boundary conditions dependent on the ratio between the servo stiffness and the normalized structural rigidity we arrived at three different models. The models are similar in that they all described the motion of the system in Fig. 1, by the rigid body motion of the structure superposed with the vibratory motion of the structure with respect to its undeformed deflection. To summarize these results consider the slope of the eigenfunction at the spring-hinged boundary. The slopes at  $x = 0$  of the eigenfunctions shown in Fig. 4 indicate the degree to which the beam is clamped (or pinned) at the slewing axis. For instance, for a high value of  $kL/EI$  the slope at the slewing axis would be nearly zero. The values of the slope of the first eigenfunction,  $(\partial \phi_1 / \partial x)(0)$ , for various values of  $kL/EI$  are plotted (see Fig. 6). These eigenfunctions are normalized as in Fig. 4 for

comparison. Some generalizations can be made from this graph and are summarized as follows.

#### Case 1: High Compliance Ratio, $kL/EI > 10$

The first model, Eq. (19), is the model of the structure shown in Fig. 1, where the vibratory motion of the beam can be described by a clamped-free beam. In this case, the stiffness coupling term  $k\Gamma_i$  approaches zero, for  $i = 1, \dots, n$ , as the compliance ratio gets larger.

#### Case 2: Moderate Compliance Ratio, $1 < kL/EI < 10$

The model is that of Eq. (19), with the additional terms of Eqs. (26) and (27), where the vibratory motion of the beam is that of a pinned/spring-free beam, so that the mode shapes and natural frequencies are similar to but slightly different than the clamped-free beam. The modal participation factors add coupling in the stiffness matrix and new terms in the control matrix.

#### Case 3: Low Compliance Ratio, $kL/EI < 1$

It has been shown that the mass matrix of Eq. (19) becomes positive semidefinite and singular. Thus, the final model is that of Eq. (19), with the redundant coordinate of the rigid body motion  $q_1$  dropped from our model. The coefficient matrices of Eq. (19) become the matrices Eqs. (31a-31d), where this model has one less degree of freedom than the models of cases 1 and 2. The values of  $kL/EI$  for the three cases are only estimations and serve only to approximate the regions of structural behavior.

### Discussion

Many experiments have been performed on the simple one-link flexible arm in Fig. 1. In modeling of these structures, investigators have assumed the clamped-free boundary conditions for the solution to the structure's vibration without considering the effects of the control on the boundary condition and thus the eigensolution of the flexible structure. The new closed-loop models of cases 2 and 3 may be of particular interest to researchers in the control of flexible structures and robotics communities who like to avoid excessive gear-trains because of the nonlinearities, such as backlash, that these often produced in experimental apparatus.

In some instances the clamped-free boundary condition assumption is valid even if the compliance ratio  $kL/EI$  is not large. Consider the case where no position control is applied, i.e., the open-loop dynamics. In all physical systems, a certain amount of deadband exists. This deadband is characterized by the amount of torque needed to overcome the friction in the motor, bearings, and gearbox. If this static friction torque is greater than the moment generated by the free vibrations of the structure about its axis, then the clamped-free eigensolution is the proper structural model. However, if the free vibrations of the structure cause rotation in the motor and gear train, then the boundary condition at the slewing axis is certainly not clamped, and it is proposed that the pinned/spring-free eigensolution is more indicative of the true structural behavior.

When discussing high gain or fast slew rate systems, the nonlinear effects of this motion acting on the beam should be considered. Effects, such as centripetal stiffening, are similar to those found in high-speed rotating structures such as helicopter blades.<sup>10,11</sup> The modeling presented in this paper is based on small vibration theory. Nonlinear considerations were beyond the scope of this work.

This work resulted from observations of two different slewing experiments, namely, the slewing apparatus in Ref. 1, located at NASA Langley's Spacecraft Dynamics Branch, and the State University of New York at Buffalo (UB) slewing experiment. The difference between the two systems is that the Langley experiment has the motor and gear train that have a static friction torque larger than the vibratory torque gener-

ated by the beam, so that the eigenfunctions of this experiment are indeed that of a clamped-free beam as defined in Ref. 1. However, the UB slewing experiment had no gear train, i.e., the motor was directly connected to the beam. The UB configuration is a low friction experiment where the vibrations of the beam cause a rotation in the motor. The proposed modeling reconciled the differences in observations between the two systems.

### Conclusions

A method for generalizing the modeling of the slewing control of flexible structures has been presented. The effects of the control on the boundary conditions have been considered, and a generalized eigensolution for controlled flexible structures in terms of the ratio between the servo stiffness and structural flexibility has been calculated. In addressing the relationship between the effect of control on boundary conditions, the presented method enables researchers to extend closed-form eigensolution of flexible beams for experiments with moderate and low compliance ratios.

### Acknowledgments

The first author gratefully acknowledges the support from NASA through the Graduate Student Research Program, Grant NGT-33183-804. The authors acknowledge the cooperation of Jer-Nan Juang of NASA Langley's Spacecraft Dynamics Branch and the grant monitor and technical advisor, Garnett C. Horner of Langley's Control-Structure Interaction Office. Additional support for the second author was also provided by the Air Force Office of Scientific Research through Grant AFOSR F49620-88-C0018.

### References

1. Juang, J.-N., Horta, L. G., and Robertshaw, H. H., "A Slewing Control Experiment for Flexible Structures," *Journal of Guidance, Control, and Dynamics*, Vol. 9, No. 5, Sept.-Oct. 1986, pp. 599-607.
2. Hastings, G. G., and Book, W. J., "A Linear Dynamic Model for Flexible Robotic Manipulators," *IEEE Control Systems Magazine*, Feb. 1987, pp. 61-64.
3. Meirovitch, L., and Juang, J.-N., "Natural Modes of Oscillation of Rotating Flexible Structures about Nontrivial Equilibrium," *Journal of Spacecraft and Rockets*, Vol. 13, No. 1, 1976, pp. 37-44.
4. Kane, T. R., Ryan, R. R., and Banerjee, A. K., "Dynamics of a Cantilever Beam Attached to a Moving Base," *Journal of Guidance, Control, and Dynamics*, Vol. 10, No. 2, 1987, pp. 139-151.
5. Breakwell, J. A., "Optimal Feedback Slewing of Flexible Spacecraft," *Journal of Guidance and Control*, Vol. 4, No. 5, 1981, pp. 472-479.
6. Book, W. J., and Majette, M., "Controller Design of Flexible, Distributed Parameter Mechanical Arms via Combined State Space and Frequency Domain Techniques," *Journal of Dynamics Measurement and Control*, Vol. 105, Dec. 1983, pp. 245-254.
7. Maizza-Neto, O., "Modal Analysis and Control of Flexible Manipulator Arms," Ph.D. Thesis, Dept. of Mechanical Engineering, MIT, Cambridge, MA, 1974.
8. Cannon, H. C., Jr., and Schmitz, E., "Initial Experiments on the End-Point Control of a Flexible One-Link Robot," *International Journal of Robotics Research*, Vol. 3, No. 3, 1984, pp. 62-75.
9. Mitchell, T. P., and Bruch, J. C., Jr., "Free Vibrations of a Flexible Arm Attached to a Compliant Finite Hub," *ASME Journal of Vibration, Acoustics, Stress and Reliability in Design*, Vol. 110, Jan. 1988, pp. 118-120.
10. Meirovitch, L., *Computational Methods in Structural Dynamics*, Sijhoff & Noordhoff, Rockville, MD, 1980, pp. 230-235.
11. Hurty, W. C., and Rubenstein, M. F., *Dynamics of Structures*, Prentice-Hall, Englewood Cliffs, NJ, 1964.
12. Inman, D. J., *Vibrations with Control, Measurement, and Stability*, Prentice-Hall, Englewood Cliffs, New Jersey, 1989.
13. Chun, K. R., "Free Vibration of a Beam with One End Spring-Hinged and Other Free," *ASME Journal of Applied Mechanics*, Vol. 39, Dec. 1972, pp. 1154, 1155.
14. Gorman, D. J., *Free Vibration Analysis of Beams and Shafts*, Wiley, New York, 1975.
15. Thomson, W. T., *Theory of Vibration with Applications*, 3rd edition, Prentice-Hall, Englewood Cliffs, NJ, 1988, p. 361.